CERN-LCGAPP-2003-18
March 9, 2004

(p,xn) Production Cross Sections: A Benchmark Study for the Validation of Hadronic Physics Simulation at LHC

Jürg Beringer
CERN
(Juerg.Beringer@cern.ch)

Abstract

As part of the physics validation effort of detector simulation tools for LHC, we study the accuracy of the simulation of double–differential (p,xn) production cross sections for thin targets of different materials at incident proton kinetic energies between 113 MeV and 800 MeV, using both Fluka and Geant4 with several physics models.

1 Introduction

The validation of the physics processes incorporated in Geant4 [1] and Fluka [2, 3], which will be the main simulation tools for the experiments being built at the Large Hadron Collider (LHC) at CERN, is very important in order to ensure that inadequate simulation models will not lead to large systematic contributions to future LHC physics results. Hadronic interactions are of particular concern, since their simulation has to rely on various models because there is no unified theory that can describe hadronic showers from first principles at all energies.

Two complementary approaches to the physics validation of simulation packages are currently pursued in the context of the LCG Simulation Physics Validation Project [4]: the comparison of simulation with test–beam results of LHC detectors for quantities such as calorimeter energy resolution or shower shape, and the study of "simple benchmark" layouts with single incident particles of various energies, where the results from simulation can be compared with experimental data from other facilities. The latter studies allow the validation of the individual microscopic interactions between incident particles and detector material.

One such simple benchmark for hadronic interactions is the simulation of neutron production from incident protons of various energies on different materials. Double–differential cross sections for this process have been measured by several groups as will be discussed below. In many cases these measurements were motivated by the goal of improving different

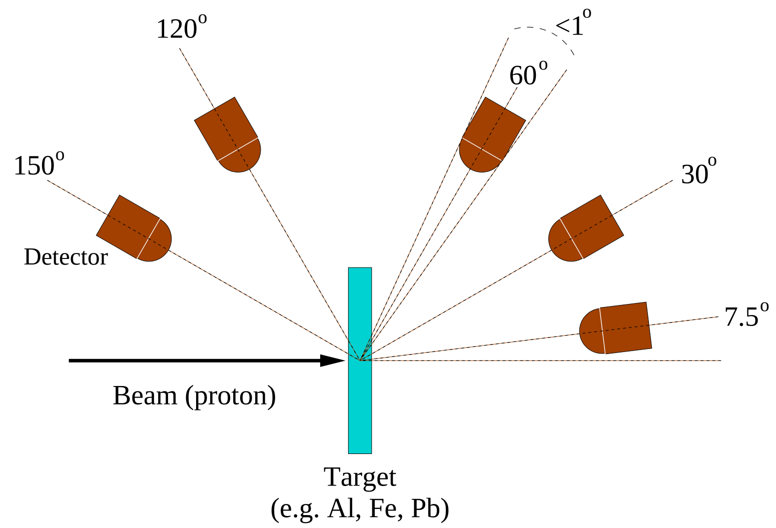

Figure 1: Sketch of the experimental setup used at Los Alamos National Laboratories for measuring double–differential neutron production cross sections (not to scale).

simulation codes. In the context of LHC, the production of low energy background neutrons is of concern for all experiments.

In this note we report results obtained from the simulation of double–differential (p,xn) production cross sections for various target materials and incident proton kinetic energies between 113 MeV and 800 MeV, using both Geant4 with several physics models and Fluka. Results from a similar study done in the context of the Alice experiment with an earlier version of Geant4 were reported in [5, 6].

1.1 Experimental Data

Double–differential (p,xn) production cross sections have been measured by several groups. Below we discuss 3 measurements we have looked at in the context of this work. For convenience, these measurements will be labelled "Los Alamos Data", "Hamburg Data", and "Saturne Data" in the following.

1.1.1 "Los Alamos Data"

Double–differential neutron production cross sections, $d^2\sigma/d\Omega dE_n$, were measured at the Los Alamos Meson Physics Facility (LAMPF) for thin targets of different materials (Be, B, C, N, O, Al, Fe, Pb and depleted uranium), at different incident proton kinetic energies $E_p = 113\,\mathrm{MeV}$, $256\,\mathrm{MeV}$, $597\,\mathrm{MeV}$, and $800\,\mathrm{MeV}$, and at different angles (7.5°, 30°, 60°, 120°, and 150°). A sketch of the experimental setup is shown in Figure 1. The results for measurements made on thin targets were published in [7, 8, 9, 10]. A related publication [11] discusses measurements of the neutron yield for stopping and near-stopping length targets for 256 MeV protons and describes the experimental setup and data analysis procedure in more detail.

All measurements were made using the time–of–flight technique with neutron detectors placed at different angles at a distance ranging from 23 m to 58 m from the target. The neutron energy resolution was better than 5% which, at the lowest proton energy $E_p = 113\,\mathrm{MeV}$,

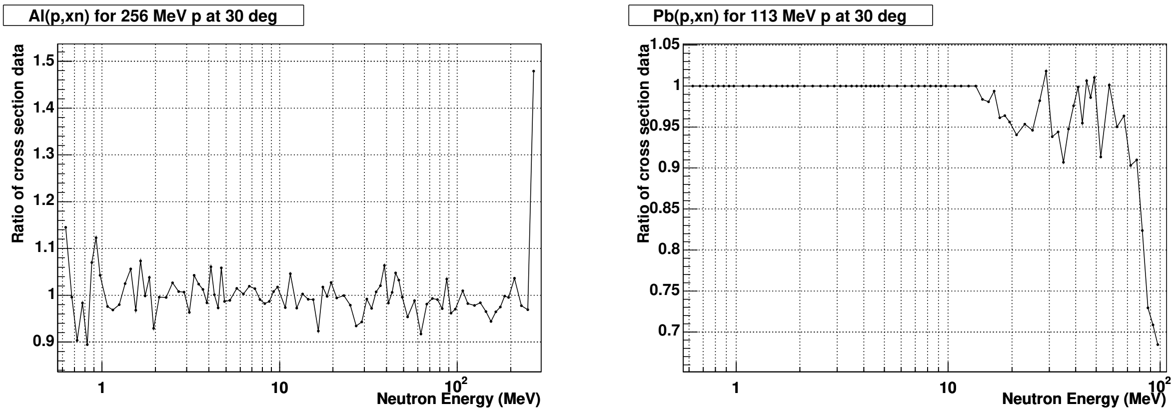

Figure 2: Examples of the level of agreement between different versions of cross section data files for the same measurement (see text). The plots show the ratio of the cross section data found in the EXFOR data files compared to the corresponding data file from [15]. The left (right) plot show the case of Al(p,xn) for 256 MeV protons at 30° (Pb(p,xn) for 113 MeV protons at 30°).

was achieved by using a dedicated setup of the Linac[1]. The neutron detectors were cylindrical BC-418 plastic scintillators with a diameter of 5.08 cm and a length of 2.54 cm (at angles of 30°, 120°, and 150°) or, for the longer (≥ 50 m) flight paths, a length of 5.08 cm (at angles of 7.5° and 60°). The neutron detector efficiencies were determined from measurements of light ion reactions as neutron sources of known intensity for neutron energies below 35 MeV [11], from a Monte–Carlo neutron detector efficiency code [12] between 35 MeV and 200 MeV, and by assuming a constant efficiency from 200 MeV up to the highest neutron energy. This data was parametrized by spline fits which, for a 5.08 cm long detector, were found to be in agreement with measurements made using monoenergetic neutrons from $^7Li(p,n)^7Be$ reactions at 0° [13, 14].

The statistical errors on the measured double-differential cross sections are below 5% for most of the neutron energy range, with larger errors near the high end of the neutron spectrum where statistics were limited. Systematic errors include contributions from background subtraction, air attenuation, detector efficiency, dead time and charge normalization. For the measurements with $E_p = 597$ MeV and 800 MeV, an additional systematic error comes from the uncertainty in the transmission through a uranium filter used to attenuate the prompt gamma flux. The total systematic error is dominated by an uncertainty of up to 20% on the neutron detector efficiency, and, for the cases where the uranium filter was used for neutron energies above 20 MeV, an uncertainty of 20% on the uranium transmission.

Two sets of data files of the measured cross sections are available: The first set [15], which was used in [5, 6], was obtained shortly after the publication of [7, 8, 9, 10] from the authors. The second set was obtained in August 2003 from the EXFOR database [16]. Apart from the addition or omission of a few data points at either the lowest or highest neutron energies, the data in the two sets of data files is identical, except for 6 cases (256 MeV protons on

[1]The maximum proton energy at LAMPF is 800 MeV. Lower proton energies were normally achieved by using only the RF cavities up to the point where the desired proton energy was reached, and the remaining ones were switched off. At 113 MeV, for a typical 1.5 MeV beam energy spread, this would result in a 39 ns bunch time spread, which would dominate the resolution of the TOF measurement. Hence a special setup of the Linac was used which reduced the time spread to a worst case of 5 ns.

aluminum at 30°, 60° and 150°, and 113 MeV protons on lead at 30°, 60° and 150°) where differences at the level of about 5% to 30% are found. Typical examples of such differences are shown in Figure 2. Because some of the data files retrieved from EXFOR contain a comment saying that in 1999 the data was replaced with corrected data, we consider the EXFOR data files to be the more accurate ones[2]. The differences between the two sets of data files are — except for a few points near the high end of the neutron spectrum — well below the systematic uncertainty of the measurement.

The errors contained in the EXFOR data files include the statistical error and the systematic errors related to background subtraction. Unfortunately, the full systematic error, and in particular the dominant one from the detector efficiency, is not available from the EXFOR database, and its neutron energy dependence could not unambiguously be determined otherwise. Therefore a conservative energy independent error of 20% was used for the contribution of the uncertainty in the neutron detector efficiency. Other contributions to the systematic error that are not already included in the data files add up to an additional systematic error of 9.4% on the cross sections for $E_p = 113$ MeV and 256 MeV, and to 10.6% and 22.1% at the higher proton energies for neutron energies below and above 20 MeV, respectively. Thus the total systematic error is in the range between 22% and 30% for all cases.

In the EXFOR data files, double–differential cross sections are given for neutron energy bins with a width of at least 5% of the central energy (i.e. the bin width is always larger than the neutron energy resolution), but the effect of the finite energy resolution was not unfolded from the measured cross sections.

1.1.2 "Hamburg Data"

Double–differential neutron production cross sections were also measured at LAMPF by a different group for incident proton energies $E_p = 256$ MeV and 800 MeV for thin Li, Al, Zr and Pb targets [17]. While the overall experimental setup was similar to the one used for the Los Alamos data, the neutron detectors used were cylindrical liquid scintillators with a diameter between 10 cm and 31 cm and a thickness between 5 cm and 20 cm (compared to the smaller plastic scintillators used for the Los Alamos measurements), and the neutron energy resolution was somewhat worse than for the Los Alamos measurements.

As in the case of the Los Alamos data, the systematic error is dominated by the uncertainty in the detector efficiency and, at the lower proton energy, by a comparable uncertainty on the attenuation in air and construction materials along the neutron flight path. The neutron detector efficiencies were determined from a Monte–Carlo neutron detector efficiency code [12] and renormalized to reference data in order to account for the fact that the code overestimates the efficiency for large detectors by 10% to 20%. The total systematic error on the double–differential cross sections is 15% for $E_p = 256$ MeV and 23% for $E_p = 800$ MeV, with contributions of 11% and 20%, respectively, from the neutron detector efficiencies.

It is well known [18] that while some of the Hamburg data is in good agreement with the Los Alamos measurements, much of the data differs by up to a factor of two. The level of agreement between the two measurements is illustraged in Figures 3 and 4, where ratios of the two measurements are shown for different cases, using the data files available from EXFOR [16] both for the Hamburg and for the Los Alamos data. The error bars shown on these plots include all statistical and systematic errors of both measurements added in

[2]We contacted the authors in order to confirm which data files are the correct ones and to find out why more than 5 years after publication a correction to their data was made. At the time of this writing we have not yet received an answer.

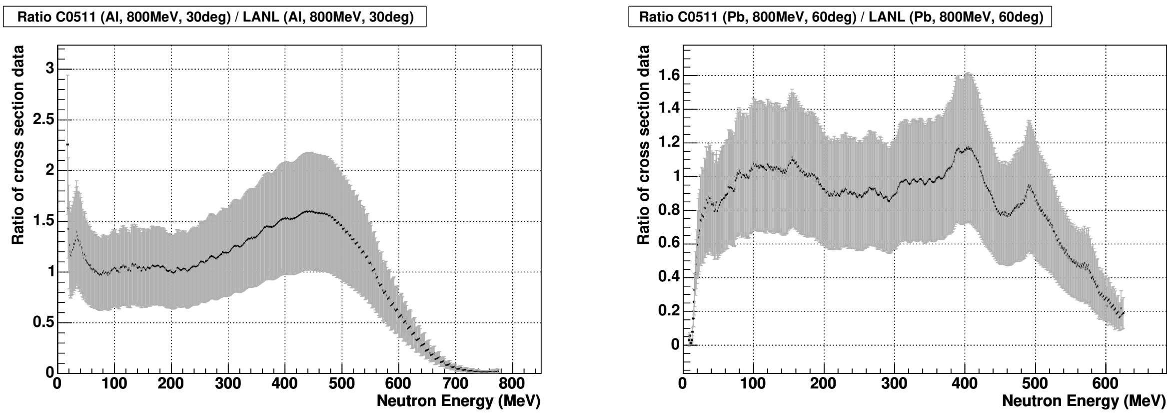

Figure 3: Ratio of double–differential neutron production cross sections measured by the Hamburg and the Los Alamos groups for two typical examples with good agreement of the data.

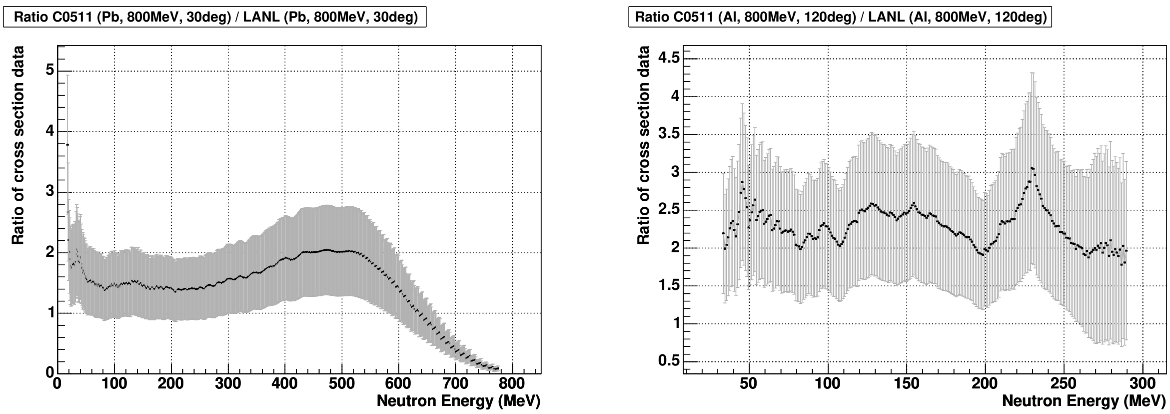

Figure 4: Ratio of double–differential neutron production cross sections measured by the Hamburg and the Los Alamos groups for two typical examples with bad agreement of the data.

quadrature, and indicate agreement at the level of one to two sigmas[3].

Given that the dominant systematic error comes from the neutron detector efficiency, one might expect an inaccurate detector calibration to be the primary source of the disagreement between the Los Alamos and the Hamburg data. Therefore the ratios of measurements made with the same pair of detectors should be identical. While in many cases one can indeed recognize a common shape of these ratios as can be seen for example by comparing the left plots on Figure 3 and 4, closer inspection of the data suggests that other factors contribute to the disagreement as well.

1.1.3 "Saturne Data"

The most recent measurements of double–differential neutron production cross sections were made at the SATURNE accelerator [19, 20]. Measurements were made with 1 cm to 3 cm thick Al, Fe, Zr, W, Pb and Th targets at incident proton energies of 0.8 GeV, 1.2 GeV and 1.8 GeV (not all materials were used at all proton energies). Low energy neutrons ($E_n \leq 400\,\mathrm{MeV}$) were measured by time of flight with an energy resolution better than 10% between 2 MeV and 400 MeV. Neutrons with an energy above 200 MeV were measured using (n,p) scattering on a liquid hydrogen converter and reconstruction of the proton trajectory in a rotating magnetic spectrometer (between 200 MeV and 400 MeV both techniques were used). Measurements of the double–differential cross section were made at different angles between 0° and 160° with systematic errors of typically less than 15%.

The authors of the Saturne data compare their results to previous measurements, including the Los Alamos Pb(p,xn) data at $E_p = 800\,\mathrm{MeV}$. When doing so, the effects of the difference of 5° to 10° in the angles where cross sections were measured, and of the difference in target thickness (a few mm for the Los Alamos data vs up to 3 cm for the Saturne data), need to be taken into account. The latter is a small effect for most cases, but for high energy neutrons the difference in angle can become quite significant as illustrated in Figure 5. For example, for 800 MeV protons on Pb one expects the cross section for the production of 400 MeV neutrons to be about 1.8 times higher at 55° than at 60°. After appropriate enlargement, this difference can be seen between the Los Alamos and the Saturne cross section data shown in Figure 2 of [19]. From Figure 5 one would also expect a difference of about 30% for 500 MeV neutrons at 25° compared to 30°, which is not present in Figure 2 of [19]. For this latter case, the Los Alamos and the Hamburg data differ significantly (see Figure 4 left plot), with the Hamburg in larger disagreement with the Saturne measurement than the Los Alamos one. For neutron energies below about 100 MeV there is almost perfect agreement between the Saturne and the Los Alamos data for 800 MeV p on Pb, and a somewhat poorer agreement for neutrons of a few MeV in the case of 800 MeV p on Fe. The latter is attributed by the authors to the difference in target thickness [20].

[3] The calculation of the error on the ratio of the Hamburg and Los Alamos measurements independently for each case (i.e. for each combination of incident proton energy, material, angle, and neutron energy) in order to determine the level of agreement of the two measurements is not strictly correct: The total error on each measurement is dominated by the systematic uncertainty on the neutron detector efficiency. The assumed neutron detection efficiency and any deviation from the correct efficiency for a given neutron energy is the same for all measurements made with the same detector at the same neutron energy, and such deviations should vary only slowly with neutron energy. The errors shown in Figures 3 and 4 neglect these correlations.

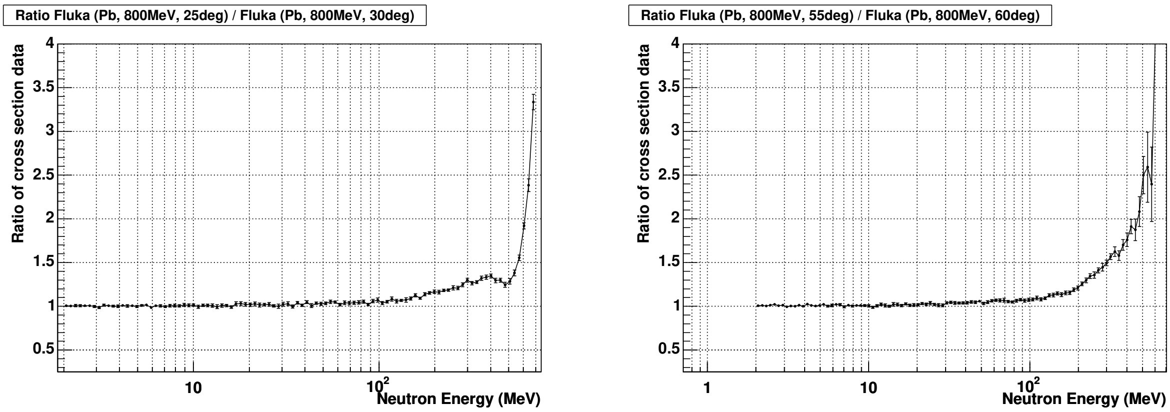

Figure 5: Effect expected from the difference in angle between the Saturne and the Los Alamos measurements of double–differential cross sections. The left (right) plot shows the ratio of the double–differential Pb(p,xn) cross sections obtained from Fluka for 800 MeV protons at angles of 25° and 30° (55° and 60°).

1.1.4 Data Used for Comparison with Simulation Results

In the present work we have concentrated on double–differential neutron production cross sections for incident proton energies up to 800 MeV. Given the good overall agreement between the Saturne and the Los Alamos data for the cases where measurements have been made by both groups, in this work we will use the Los Alamos data for comparing simulated double–differential cross sections to experimental data.

2 Simulation Setup

We have used both Geant4 and Fluka in order to simulate double–differential neutron production cross sections. While the physics algorithms and models used by Fluka [2, 3] are fixed and cannot be influenced by the user apart from enabling or disabling certain processes and changing parameters such as cutoff energies, Geant4 gives the user complete freedom as to what physics algorithms to use and does not provide a default physics model. Instead, the user chooses the desired algorithms by creating a phyiscs list that specifies how electromagnetic and hadronic interactions should be modelled. In the following, in addition to Fluka, we will use Geant4 with the following physics lists [21]:

- **LHEP** uses low energy and high energy parametrized models that are applied in their respective area of validity. It is one of the fastest models of hadronic interactions and is loosely based on the Gheisha package of Geant3.

- **QGSP_BERT** uses theory driven modeling for the reactions of energetic pions, kaons, and nucleons. The quark gluon string model, together with the corresponding string fragmentation function, is used to model the initial "punch-through" interaction of the projectile with a nucleus. A pre-equilibrium decay model with an extensive evaporation phase is used to model the nuclear fragmentation that occures after the initial soft interaction, and to describe the evolution of the nucleus. Below 3 GeV kinetic energy the classical Bertini Cascade is used for nucleon and pion induced reactions. The physics list uses the Wellisch-Axen systematics for the calculation of nuclear reaction

	Version
Thin target benchmark code	ThinTarget-1-0-0
Fluka	2002.4
Geant4 release	5.2.p01
Geant4 common physics list code (PACK)	2.1
Geant4 LHEP physics list	equivalent to 3.6
Geant4 QGSP_BERT physics list	0.5
Geant4 QGSP_BIC physics list	0.5
ROOT	3.10.01
CLHEP	1.8.0.0
gcc	3.2

Table 1: Software versions used for the results presented in this note.

cross-sections at energies below about 10 GeV. Gamma and electro nuclear physics are not modelled. In all areas not specifically described, parametrized models are used. For the purpose of this note, the essential feature of this physics list is the Bertini Cascade.

- **QGSP_BIC** is similar to the QGSP_BERT physics list, except that below a kinetic energy of 3 GeV a Binary Cascade model, which is a hybrid between a generalized classical cascade and a quantuum molecular dynamics model, is used instead of the Bertini Cascade.

Further information on the Geant4 physics lists can be found in [1, 21, 22] and references therein.

This note is concerned with neutron production in thin targets, where, by definition, the probability of a hadronic interaction of the incoming particle with a nucleus of the target material is small. The simulation of such processes can be sped up greatly by using a setup where only the desired interactions are allowed and other processes such as dE/dx are not simulated. In Geant4 this can be achieved by using a large volume filled with the target material and by enabling only particle transportation and hadronic interactions. During the simulation of each event one waits for the desired hadronic interaction to take place, analyzes the interaction products, and then discards the event. For Fluka, one can use an alternate event loop routine that must be obtained directly from the Fluka authors and forces the desired hadron–nucleus interactions to occur[4].

The results presented in this note were produced using the software versions indicated in table 1. The Geant4 user code, scripts to run Geant4 and Fluka, as well as ROOT macros to analyze the results and create plots, are available in the CVS repository of the LCG Simulation Project. Instructions on how to run the code and redo these studies, for example in order to validate future versions of Geant4 or Fluka, can be found in [23].

[4]The source code for this bypass routine (and for any other part of Fluka) is not public. We checked for one case that the results obtained with this special event loop routine is compatible with the results obtained from the non–optimized simulation of a thin slab of material.

3 Results

In this section we discuss the results obtained from the simulation of (p,xn) production cross sections using Geant4 and Fluka. Among the large number of combinations of incident proton energy, material and angles one could look at, we chose to concentrate on 3 materials (Al, Fe and Pb) and the angles and incident proton energies for which measurements were made by the Los Alamos group. All comparisons with experimental data shown in the following are based on the Los Alamos data [7, 8, 9, 10] as discussed above.

The error bars in the plots shown in the following include the statistical and systematic errors on the experimental data as discussed in section 1.1.1, and a comparatively small statistical error on the simulated results. Where ratios of simulated to experimental cross sections are shown, the experimental data was linearly interpolated to the bin centers chosen for the simulation.

Although the effect of the finite energy resolution is folded into the experimentally measured double–differential cross sections, we did not convolute the simulated cross sections with a similar neutron energy resolution function. Given that there are no narrow resonances for the cases considered and that the widths of the neutron energy bins are anyway larger than the experimental energy resolution, such a convolution would have a small effect and would not change any of our conclusions.

In the following, we will show only a small number of representative plots selected from the large number of comparisons made for the different combinations of incident proton energy, material, angle, and simulation model. Plots for all the other cases can be found on the web pages [23] of the LCG Simulation Physics Validation Project.

3.1 Double–Differential Cross Sections

An example of the level of agreement between simulated and exerimental double–differential neutron production cross sections is shown in Figure 6 for 256 MeV protons on iron at an angle of 30°.

With the exception of the LHEP physics list, which, being a parametrized model, is not suitable for this kind of studies, both the Bertini and the Binary Cascade models as implemented in the Geant4 QGSP_BERT and QGSP_BIC physics lists as well as Fluka can reproduce the overall shape and magnitude of the double–differential cross sections. Figures 7, 8 and 9, which give a closer look at the ratios between the simulated and the experimental data shown in Figure 6 (Fe(p,xn) for 256 MeV protons at 30°), show that the agreement of simulation with experimental data is typically at the level of 20% to 50%, corresponding to about one to two times the combined statistical and systematic error on the ratio between simulation and data.

Further examples are shown for Al(p,xn) at $E_p = 113\,\mathrm{MeV}$ and for Pb(p,xn) at $E_p = 800\,\mathrm{MeV}$ in Figures 10 and 11. The corresponding plots of the ratios between simulation and experimental data are shown in Figures 12 and 13 for Fluka, in Figures 14 and 15 for the QGSP_BERT physics list, and in Figures 16 and 17 for the QGSP_BIC physics list. In the case of the QGSP_BIC physics list one can recognize a discontinuity in the double–differential cross section at a neutron energy of about 70 MeV for Pb(p,xn) at $E_p = 800\,\mathrm{MeV}$, which is most pronounced at low angles. The same discontinuity appears also at $E_p = 597\,\mathrm{MeV}$. This is a consequence of the way the transition from cascade to precompound is implemented in the QGSP_BIC physics list. This problem should be fixed in the next release of Geant4.

Apart from the discontinuity problem mentioned above, the overall level of agreement

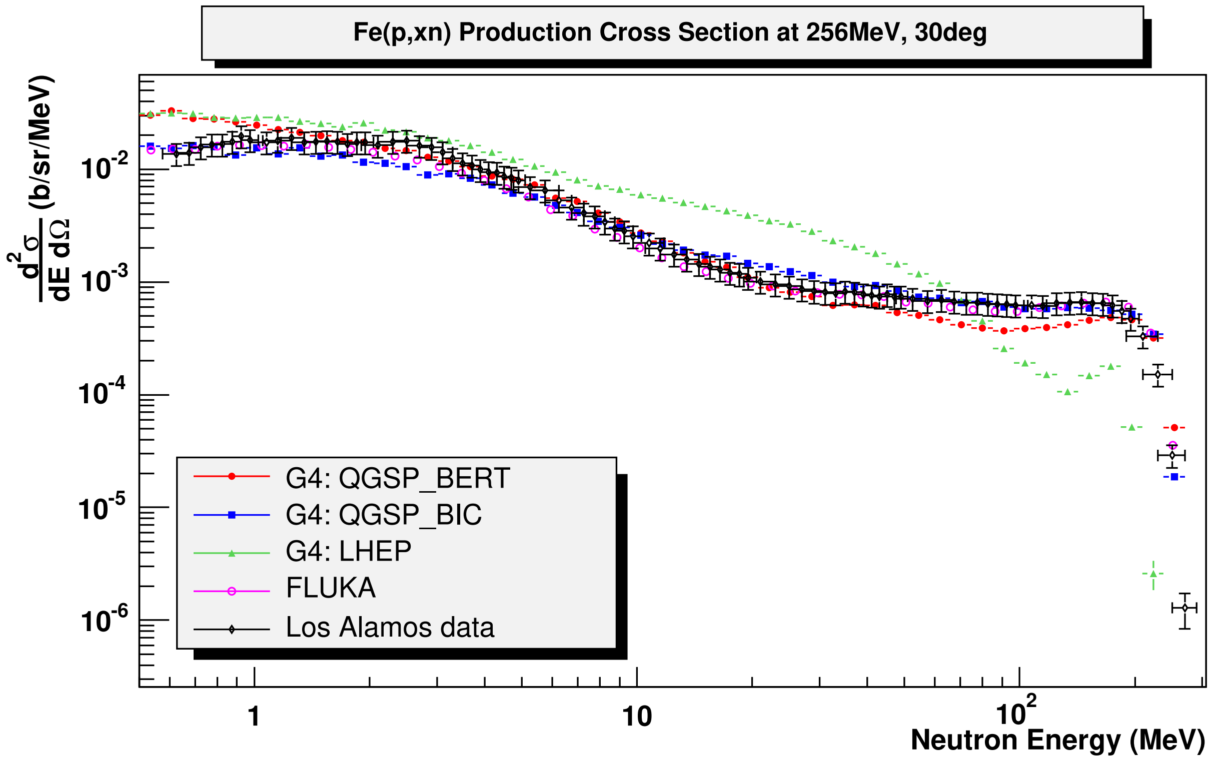

Figure 6: Double–differential Fe(p,xn) production cross sections for 256 MeV protons at an angle of 30°.

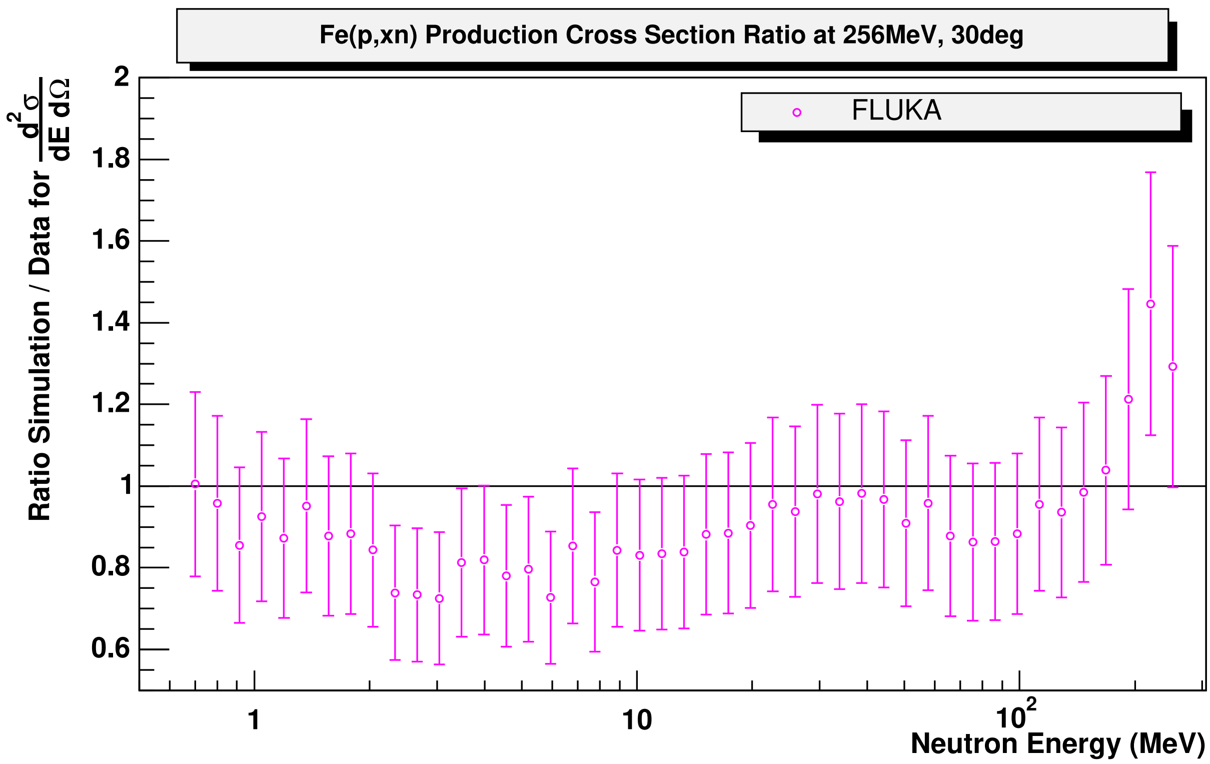

Figure 7: Ratio of simulated to experimental cross sections for the Fluka physics list for the data shown in figure 6 (Fe(p,xn) for 256 MeV protons at 30°).

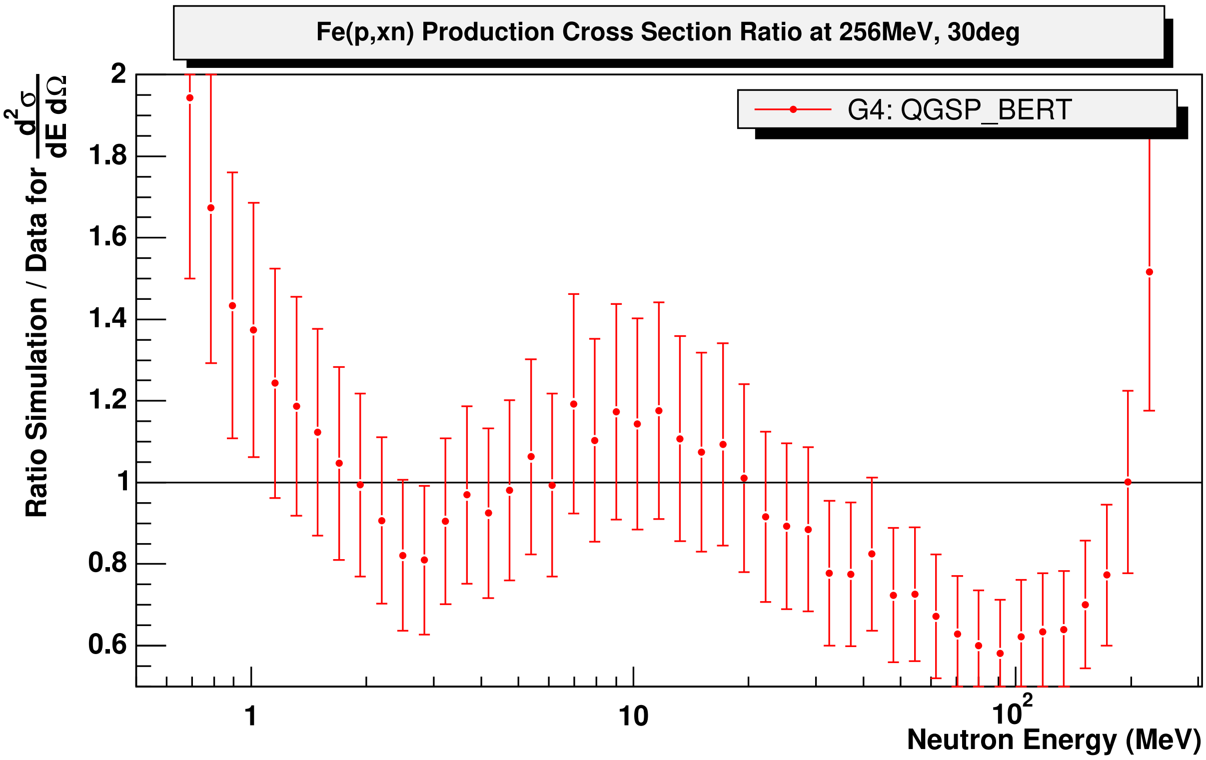

Figure 8: Ratio of simulated to experimental cross sections for the QGSP_BERT physics list for the data shown in figure 6 (Fe(p,xn) for 256 MeV protons at 30°).

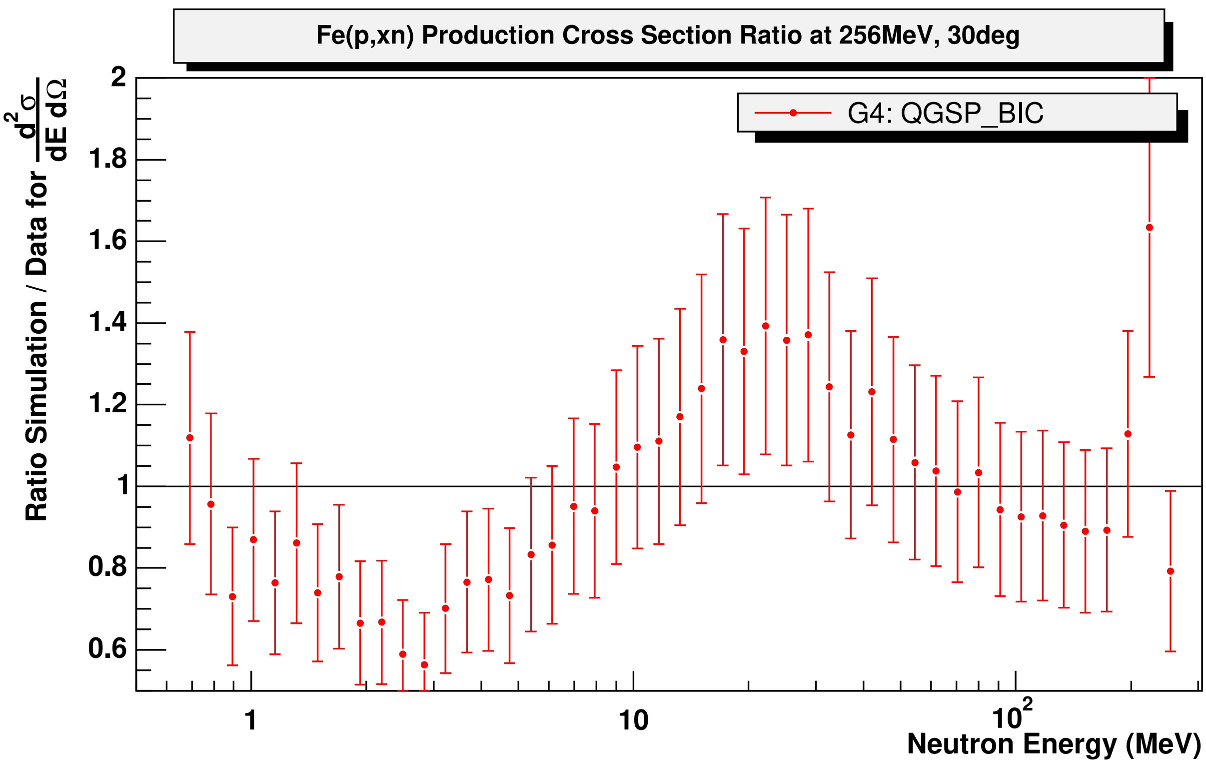

Figure 9: Ratio of simulated to experimental cross sections for the QGSP_BIC physics list for the data shown in figure 6 (Fe(p,xn) for 256 MeV protons at 30°).

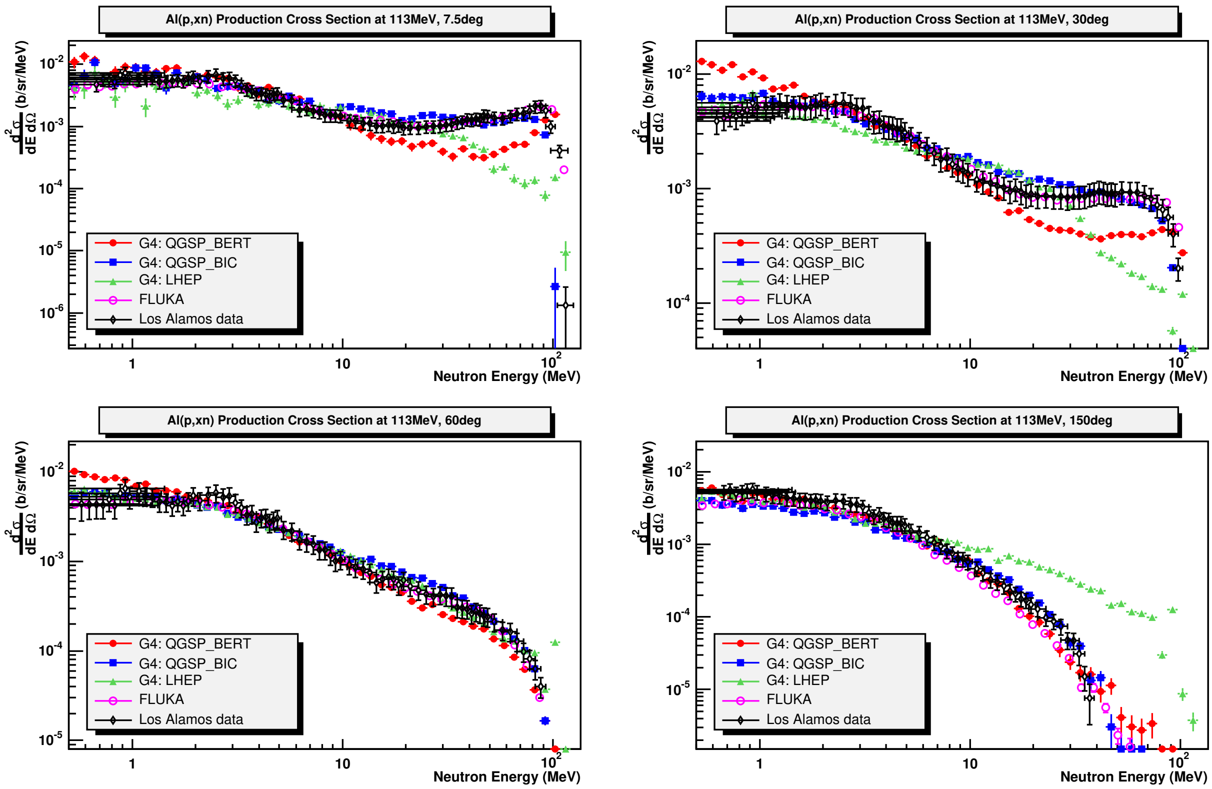

Figure 10: Double–differential Al(p,xn) production cross sections for 113 MeV protons.

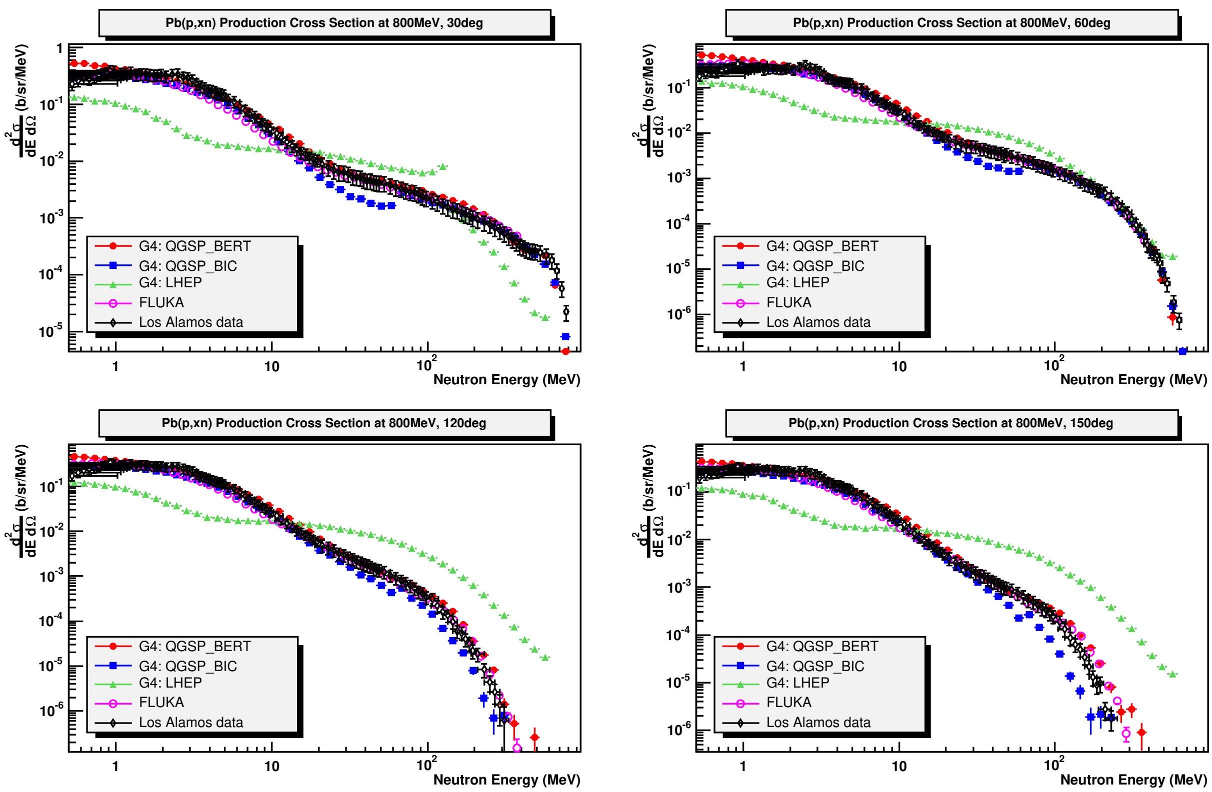

Figure 11: Double–differential Pb(p,xn) production cross sections for 800 MeV protons.

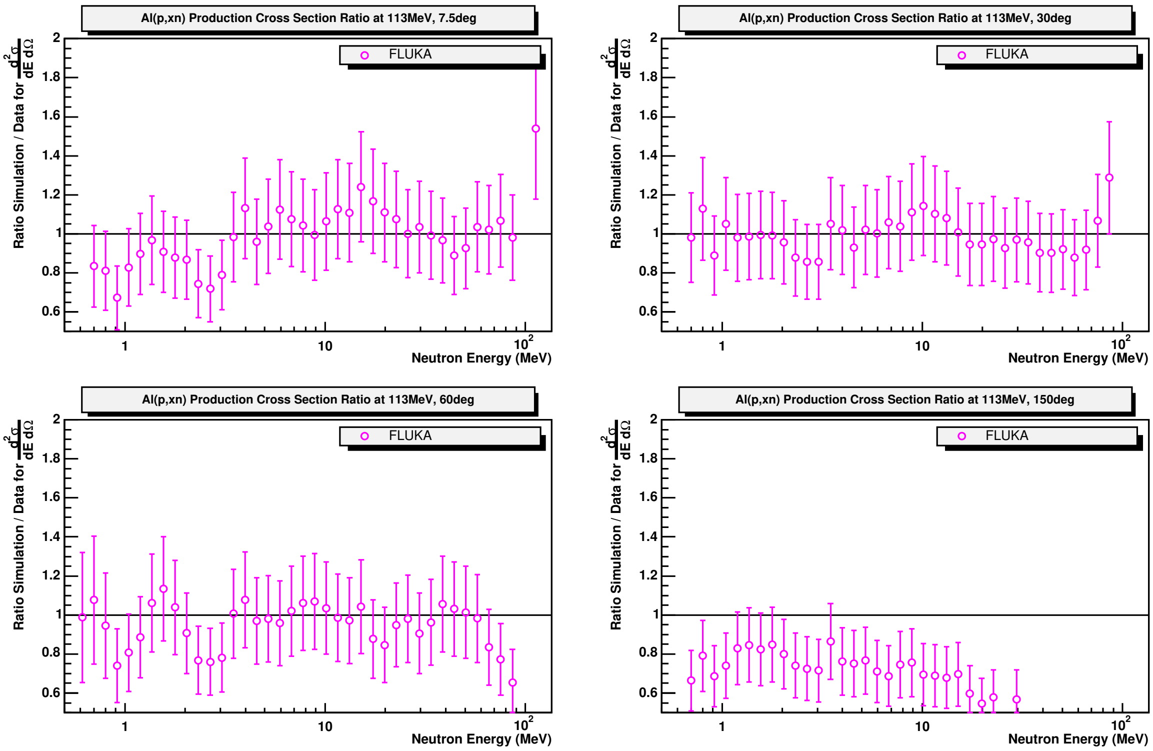

Figure 12: Ratio of simulated to experimental cross sections for Fluka for the data shown in Figure 10 (Al(p,xn) for 113 MeV protons).

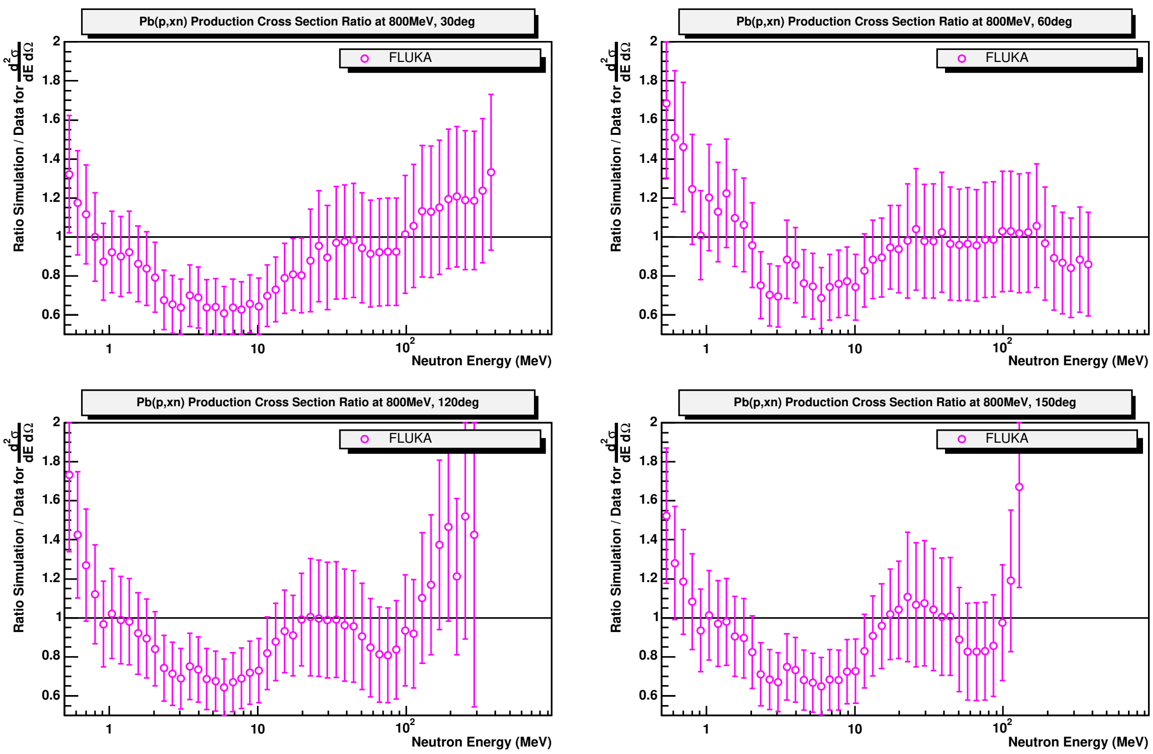

Figure 13: Ratio of simulated to experimental cross sections for Fluka for the data shown in Figure 11 (Pb(p,xn) for 800 MeV protons).

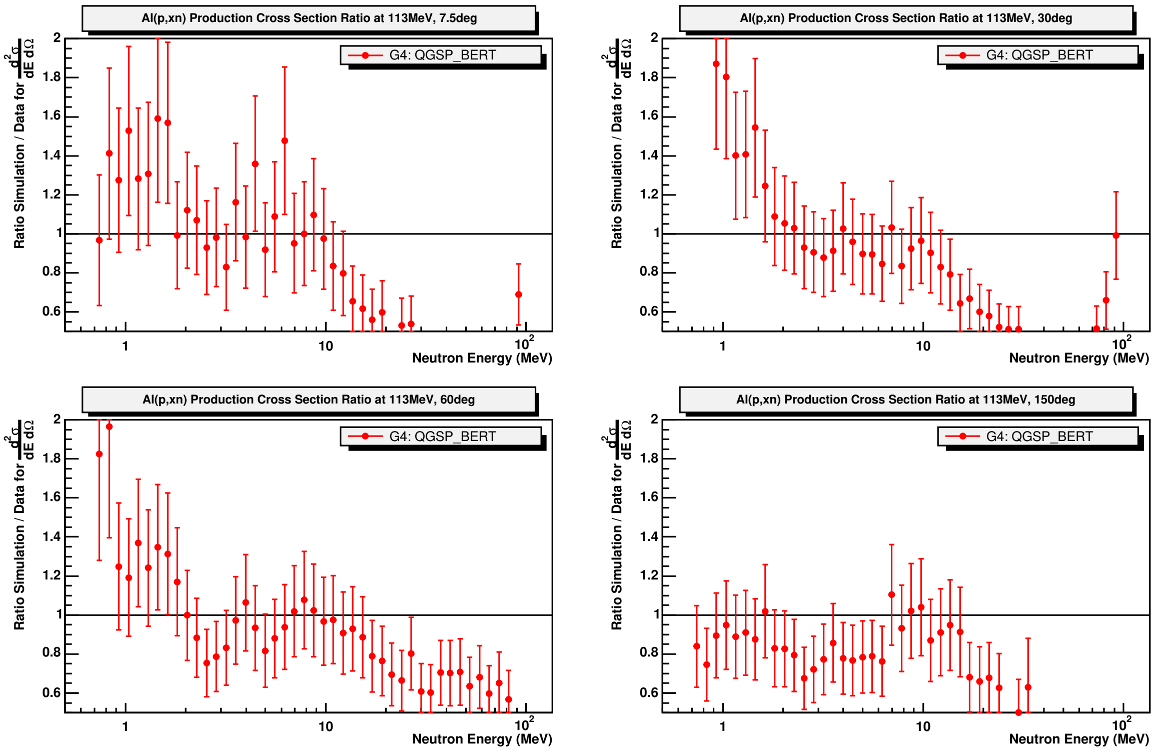

Figure 14: Ratio of simulated to experimental cross sections for QGSP_BERT physics list for the data shown in Figure 10 (Al(p,xn) for 113 MeV protons).

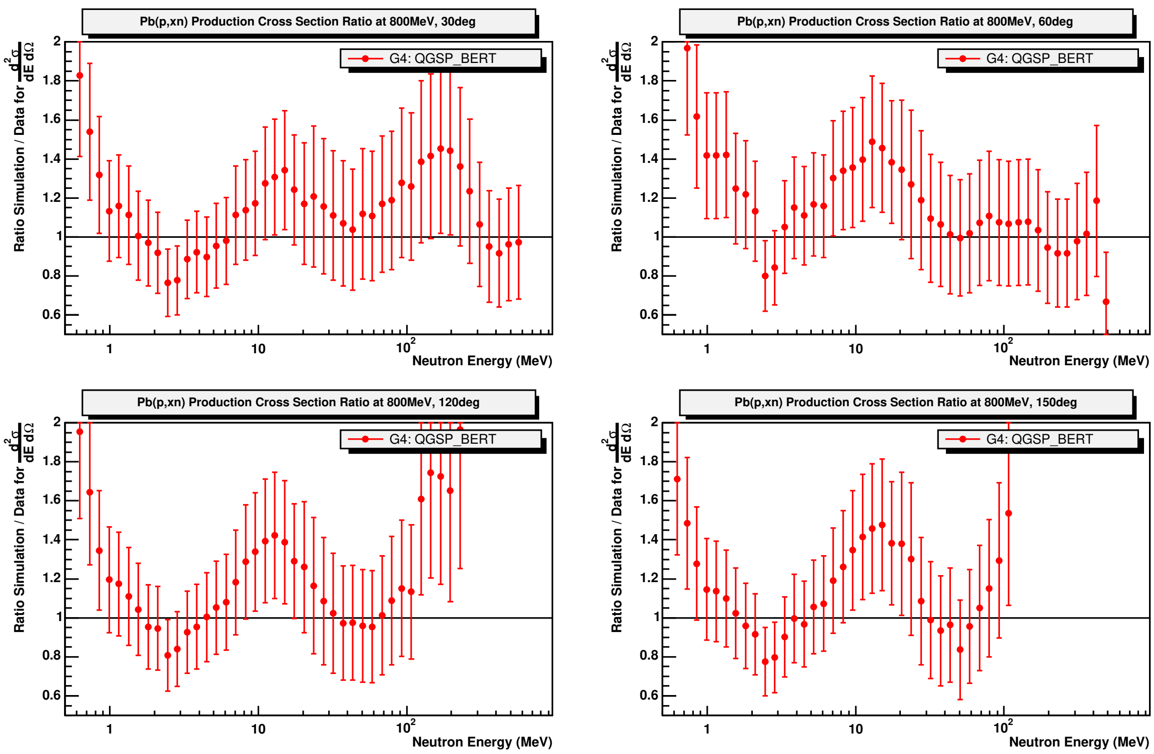

Figure 15: Ratio of simulated to experimental cross sections for QGSP_BERT physics list for the data shown in Figure 11 (Pb(p,xn) for 800 MeV protons).

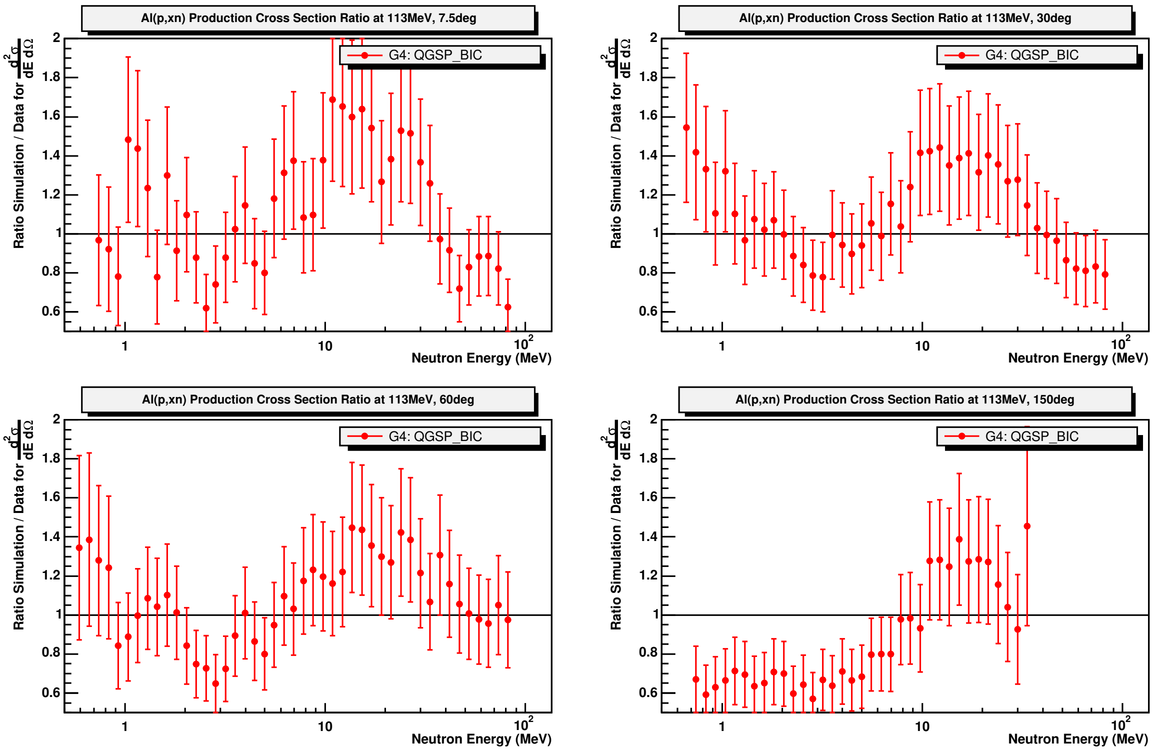

Figure 16: Ratio of simulated to experimental cross sections for QGSP_BIC physics list for the data shown in Figure 10 (Al(p,xn) for 113 MeV protons).

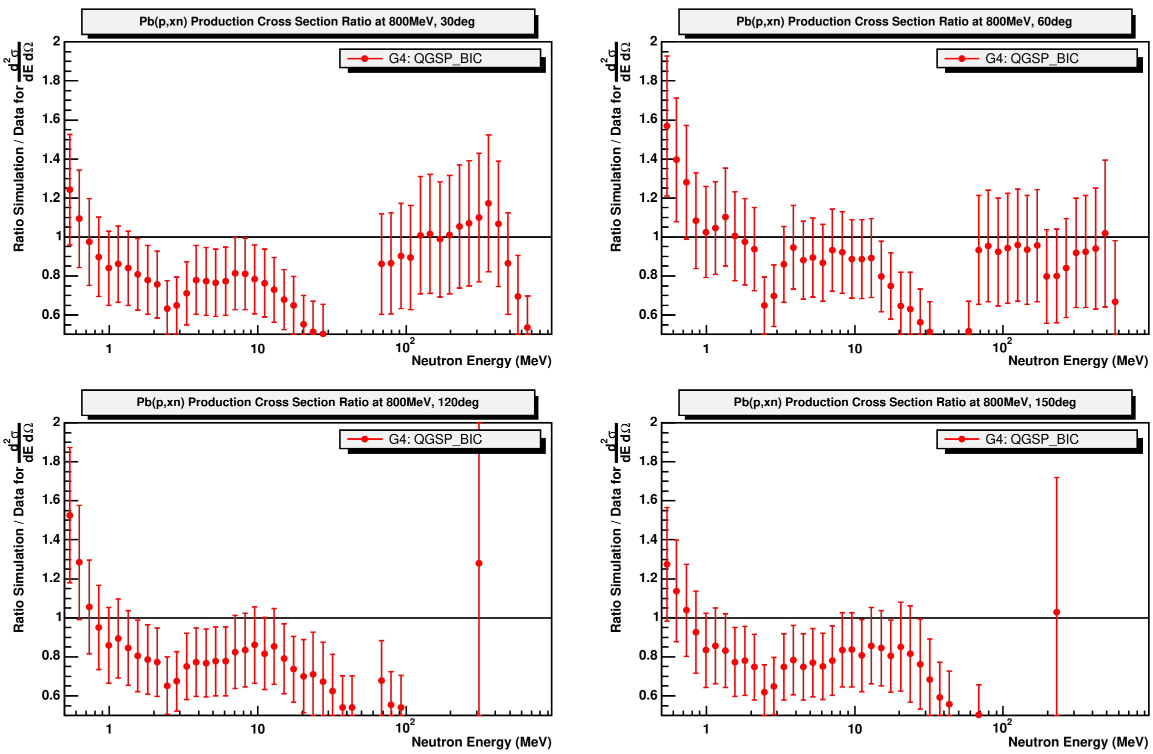

Figure 17: Ratio of simulated to experimental cross sections for QGSP_BIC physics list for the data shown in Figure 11 (Pb(p,xn) for 800 MeV protons).

of Geant4 and Fluka with experimental data is quite comparable. In some cases, such as Fe(p,xn) for 256 MeV protons at 30° (Figures 7 – 9), Geant4 shows strong variations with neutron energy of the ratio between simulated and experimental cross sections, while Fluka is merely shifted up or down, but similar variations with neutron energy can be found also for Fluka, for example in the case of Pb(p,xn) for 800 MeV protons (Figure 13).

3.2 Cross Checks

While the emphasis of our studies was to simulate double–differential neutron production cross sections and to compare them with experimental data, a number of cross checks such as the azimuthal distributions of emitted neutrons, protons and pions were done for the QGSP_BERT and QGSP_BIC physics lists. Plots from these studies can be found on [23]. No problems were found for the QGSP_BERT physics list, but in the case of the QGSP_BIC physics list it was discovered that in a certain fraction of events (0.5% in the case of Al(p,xn) at $E_p = 113\,\mathrm{MeV}$) neutrons are emitted unphysically with zero momentum in the laboratory frame. A similar problem of pions being produced at rest was observed too, albeit in a smaller fraction of events. This problem should also be fixed in the next release of Geant4.

4 Conclusions

We have used both Geant4 and Fluka to simulate the production of neutrons from incident protons with kinetic energies between 113 MeV and 800 MeV on thin Al, Fe and Pb targets. Comparison of the simulated double-differential cross sections with experimental data measured at the Los Alamos National Laboratory shows agreement typically at the level of 20% to 50%, corresponding to about one to two times the combined statistical and systematic error on the ratio between simulation and data. The accuracy of these comparisons is to a large extent limited by the systematic errors of up to 30% on the available experimental data.

Overall, the level of agreement of Geant4 and Fluka with the experimental data was found to be comparable, although Geant4 shows a somewhat more pronounced variation with neutron energy of the ratio between simulated and experimental double–differential cross sections than Fluka. Compared to a similar study [5, 6] done previously using an older version of Geant4, an impressive improvement is observed in the accuracy with which Geant4 can model such processes.

The code that has been developed to do the studies described in this note is available from the CVS repository of the LCG Simulation Project and instructions for its use can be found on [23]. The code can be used to quickly redo these studies with upcoming versions of Geant4 and Fluka. Beyond that, the code developed for Geant4 is sufficiently general that many similar thin target benchmark studies can be done with a minimum amount of effort.

Acknowledgements

It is a pleasure to thank John Apostolakis, Federico Carminati, Andrea Dell'Acqua, Alfredo Ferrari, Fabiola Gianotti, Andreas Morsch, Paola Sala and Hans–Peter Wellisch for many useful discussions and suggestions. We thank Isidro Gonzalez for providing some code as a starting point for this work.

References

[1] S. Agostinelli et al., *Geant4 — A Simulation Toolkit*, Nucl. Instr. and Meth. **A506** (2003) 250

[2] A. Fasso, A. Ferrari, and P.R. Sala, *Electron-photon transport in FLUKA: Status*, Proceedings of the MonteCarlo 2000 Conference (Lisbon, October 23-26, 2000), eds A. Kling et al., Springer-Verlag Berlin, p. 159-164 (2001)

[3] A. Fasso et al., *FLUKA: Status and Prospective for Hadronic Applications*, Proceedings of the MonteCarlo 2000 Conference (Lisbon, October 23-26, 2000), eds A. Kling et al., Springer-Verlag Berlin, p. 955-960 (2001)

[4] Physics Validation Project, `http://lcgapp.cern.ch/project/simu/validation/`

[5] F. Carminati and I. Gonzalez-Caballero, *Geant4: A Benchmark of Hadronic Processes*, ALICE-INT-2001-041

[6] ALICE Collaboration (I. Gonzalez Caballero et al.), *ALICE EXPERIENCE WITH GEANT4*, Proceedings of 2003 Conference for Computing in High-Energy and Nuclear Physics (CHEP 03), La Jolla, California, 24-28 Mar 2003

[7] M.M. Meier et al., *Differential Neutron Production Cross Sections and Neutron Yields from Stopping-Length Targets for 113MeV Protons*, Nucl Sci Eng 102 (1989) 310-321

[8] M.M. Meier et al., *Differential Neutron Production Cross Sections for 256MeV Protons*, Nucl Sci Eng 110 (1992) 289-298

[9] W.B. Amian et al., *Differential Neutron Production Cross Sections for 597MeV Protons*, Nucl Sci Eng 115 (1993) 1-12

[10] W.B. Amian et al., *Differential Neutron Production Cross Sections for 800MeV Protons*, Nucl Sci Eng 112 (1992) 78-86

[11] M.M. Meier et al., *Neutron Yields from Stopping- and Near-Stopping-Length Targets for 256MeV Protons*, Nucl Sci Eng 104 (1990) 339-363

[12] R. A. Cecil et al., *Improved predections of neutron detection efficiency for hydrocarbon scintillators from 1 MeV to about 300 MeV*, Nucl Instr Meth 161 (1979) 439-447

[13] W. B. Amian et al., *Efficiency calibration of a cylindrical BC418 neutron detector at neutron energies between 30 and 200 MeV*, Nucl Instr Meth A281 (1989) 353-358

[14] W. B. Amian et al., *Efficiency calibration of a cylindrical BC418 neutron detector at neutron energies between 135 and 800 MeV*, Nucl Instr Meth A313 (1992) 452-456

[15] Alfredo Ferrari, private communication

[16] EXFOR: Experimental Nuclear Reaction Data Retrievals, `http://www.nea.fr/html/dbdata/x4/welcome.html`

[17] S. Stamer et al., *Double differential cross sections for neutron emission induced by 256 MeV and 800 MeV protons*, Phys Rev C47, 1647-1658 (1993)

[18] M. Blann et al, Nuclear Energy Agency, *International Code Comparison for Intermediate Energy Nuclear Data*, OECD 1994

[19] X. Ledoux et al., *Spallation Neutron Production by 0.8, 1.2 and 1.6 GeV Protons on Pb Targets*, Phys. Rev. Lett. 82 (1999) 4412

[20] S. Leray et al., *Spallation neutron production by 0.8, 1.2, and 1.6 GeV protons on various targets*, Phys. Rev. C 65, 044621 (2002)

[21] J.P. Wellisch, *Educated Guess Physics Lists for Geant4 Hadronic Physics*, `http://cmsdoc.cern.ch/h̃pw/GHAD/HomePage/`

[22] Geant4 Collaboration, *Physics Reference Manual*, available from `http://geant4.web.cern.ch/geant4/G4UsersDocuments/Overview/html/index.html`

[23] J. Beringer, *Simple Benchmarks: (p,xn) Production Cross Sections*, `http://lcgapp.cern.ch/project/simu/validation/benchmarks/neutron/index.html`